ELSEVIER

Journal of Nuclear Materials 283–287 (2000) 334–338

journal of nuclear materials

www.elsevier.nl/locate/jnucmat

Swelling of F82H irradiated at 673 K up to 51 dpa in HFIR

Y. Miwa [a,*], E. Wakai [a], K. Shiba [a], N. Hashimoto [b], J.P. Robertson [b], A.F. Rowcliffe [b], A. Hishinuma [a]

[a] *Department of Materials Science, Japan Atomic Energy Research Institute, Tokai-mura, Naka-gun, Ibaraki-ken 319-1195, Japan*
[b] *Metals and Ceramics Division, Oak Ridge National Laboratory, Oak Ridge, TN 37831-6376, USA*

Abstract

Reduced-activation ferritic/martensitic steel, F82H (8Cr–2W–0.2V–0.04Ta–0.1C), and variants doped with isotopically tailored boron were irradiated at 673 K up to 51 dpa in the high flux isotope reactor (HFIR). The concentrations of ^{10}B in these alloys were 4, 62, and 325 appm during HFIR irradiation which resulted in the production of 4, 62 and 325 appm He, respectively. After irradiation, transmission electron microscopy (TEM) was carried out. The number density of cavities increased and the average diameter of cavities decreased with increasing amounts of ^{10}B. The number density decreased and the average diameter increased with increasing displacement damage. Swelling increased as a function of displacement damage and He concentration.

1. Introduction

Reduced-activation ferritic/martensitic steel, F82H (8Cr–2W–0.2V–0.04Ta–0.1C), is recognized as a leading candidate for the first wall structure of future fusion reactors [1]. The structural materials of D–T fusion reactors will undergo high displacement damage and helium and hydrogen gas generation by 14.1-MeV neutrons. Because simultaneous helium gas generation with displacement damage has a strong influence on microstructures and mechanical properties of materials, irradiation experiments using boron and/or nickel-doped materials in mixed spectrum reactors have been carried out to simulate the influence of helium generation [2,3]. Irradiation of ^{10}B-doped alloys in a mixed spectrum reactor results in the transmutation of ^{10}B to He, allowing for the production of helium, and displacement damage in these alloys.

To study the effects of helium generation and displacement damage during neutron irradiation, the amount of ^{10}B in the F82H was varied. The effects of displacement damage and helium generation on the swelling behavior of F82H are presented.

2. Experimental procedure

Standard F82H (F82H-std) and variants doped with isotopically tailored boron were used for the irradiation experiment. The concentration of ^{10}B in the F82H std was about 4–8 appm, and the concentrations in alloys doped with isotopically tailored boron, F82H-2 and F82H-3, were about 62 and 325 appm, respectively. The chemical compositions are listed in Table 1.

The alloys were austenitized for 0.5–0.667 h at 1313 K and then air-cooled. Tempering treatments were carried out for 1.5–2 h at 1013 K and then air-cooled. Standard transmission electron microscopy (TEM) disks 3 mm in diameter and 0.25 mm in thickness were cut from plates of these alloys.

TEM disks were irradiated at about 673 K to dose levels of about 7.4 [4], 26 and 51 dpa [5] in a target position of the high flux isotope reactor (HFIR). After irradiation in HFIR to 1 dpa, 99.8% of ^{10}B was burned up. Therefore, 4–8, 62 and 325 appm He were introduced at about 1 dpa in F82H-std, F82H-2 and F82H-3, respectively. Helium was also generated from other transmutation reactions such as ^{56}Fe(n,α)^{53}Cr. This

* Corresponding author. Tel.: +81-29 282 6082; fax: +81-29 282 6122.
E-mail address: miway@popsvr.tokai.jaeri.go.jp (Y. Miwa).

0022-3115/00/$ - see front matter
PII: S0022-3115(00)00222-1

Table 1
Chemical compositions (mass %)

ID	C	Si	Mn	P	S	Cr	W	V	Ta	Al	N	Ni	Ti	B
F82H-std	0.097	0.09	0.07	0.002	0.003	7.46	2.1	0.18	0.03	0.014	0.004	0.03	0.008	0.0004[a]
F82H-std	0.100	0.14	0.49	0.001	0.001	7.44	2.0	0.20	0.04	0.019	0.002			0.0008[a]
F82H-2	0.099	0.15	0.5	0.001	0.001	7.49	2.1	0.20	0.04	0.021	0.001			0.0060[a]
F82H-3	0.098	0.17	0.5	0.001	0.001	7.23	2.1	0.22	0.04	0.021	0.002			0.0058[b]

[a] Natural boron; 4 or 8 appm ^{10}B in F82H-std and 62 appm ^{10}B in F82H-2.
[b] All boron is ^{10}B; 325 appm ^{10}B in F82H-3.

additional He generation rate is approximately 0.32 appm He/dpa. The dose dependence of the calculated He concentration in these alloys is shown in Fig. 1(h). After irradiation, the microstructures of these specimens were examined using a JEM-2000FX electron microscope.

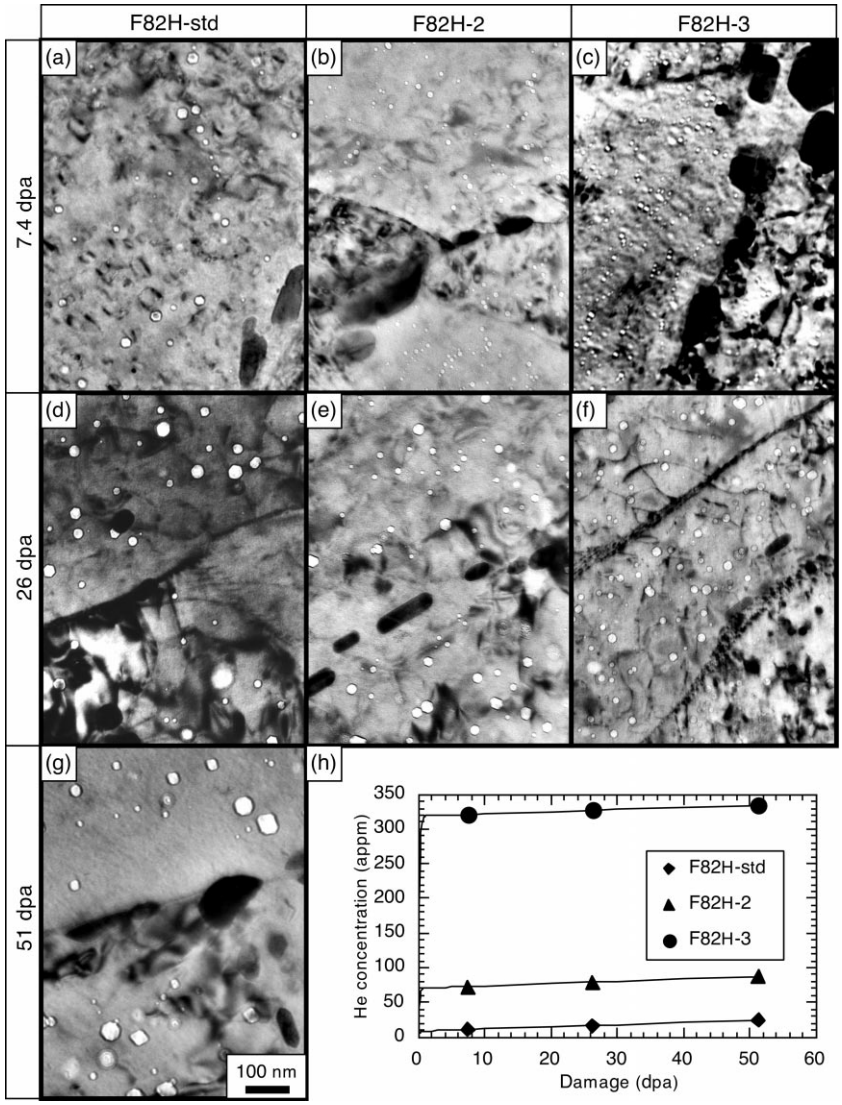

Fig. 1. Cavity microstructure ((a)–(g)) observed in F82H-std (4.1 or 8.2 appm ^{10}B), F82H-2 (62 appm ^{10}B) and F82H-3 (325 appm ^{10}B) irradiated at 673 K up to 51 dpa in HFIR. Bimodal size distributions of cavities were observed in (a), (b), (d), (e) and (f). Fig. 1(h) shows the dose dependence of helium concentration in these alloys.

3. Results

3.1. Microstructure of alloys irradiated to 7.4 dpa

Fig. 1(a)–(c) show the cavities in F82H-std, F82H-2 and F82H-3 irradiated at 673 K to 7.4 dpa. In F82H-std and F82H-2, small spherical cavities with diameters of 2–3 nm, and large faceted cavities were observed. The smaller cavities are probably He bubbles and the larger cavities are probably voids. The size distribution of cavities in these alloys was bimodal. The upper cut-off diameter for smaller cavities or the critical diameter, was about 5 nm. Because of the difficulty in TEM observations of small cavities, the number densities of He bubbles in F82H-std and F82H-2 were approximate but of the same order as that of the number densities of voids (N_v). The size distribution of voids in these alloys had a peak at 7–8-nm diameter, and the maximum diameters of the F82H-std and F82H-2 were 23 and 20 nm, respectively. The volume-averaged diameters of the voids (d^V_{RMC}) in F82H-std and F82H-2 were 9.6 and 9.2 nm, respectively. The N_v in F82H-std and F82H-2 were about 8.1×10^{20} and 2.6×10^{21} m^{-3}, respectively. Swellings in F82H-std and F82H-2 were about 0.038 and 0.11%, respectively. In F82H-3, the size distribution of cavities had a peak at 4-nm diameter, and the maximum diameter was 17 nm. The volume-averaged diameter of cavities (d^C_{RMC}) was 6.3 nm. The number density of cavities in F82H-3 was about 1.1×10^{22} m^{-3}. Swelling was about 0.14%.

In F82H-std and F82H-2, voids were frequently observed on dislocation lines. Helium bubbles were also observed preferentially on dislocation lines, and some He bubbles were observed on dislocation loops. Voids and He bubbles observed between the dislocation lines seemed to be arranged in rows. No voids were observed on lath boundaries. In F82H-3, cavities were formed uniformly. A few cavities were observed on lath boundaries. In all the alloys, the number density of cavities in the region around the lath boundaries was lower than that in the center region of lath cells.

3.2. Microstructures of alloys irradiated to 26 dpa

Fig. 1(d)–(f) show the cavities in F82H-std, F82H-2 and F82H-3 irradiated at 673 K to 26 dpa. In all alloys, small spherical cavities and large faceted cavities were observed. The size distribution of cavities was bimodal. The d^V_{RMC} and N_v in F82H-std, F82H-2 and F82H-3 were 17.2 nm and 5.6×10^{20} m^{-3}, 15.9 nm and 1.5×10^{21} m^{-3}, and 12.3 nm and 3.8×10^{21} m^{-3}, respectively. The size distribution of voids in all alloys had a peak at 9–10-nm diameter, and the maximum diameters in F82H-std, F82H-2 and F82H-3 were 43 nm, 32 nm, and 28 nm, respectively. The critical diameter of He bubbles was about 6 nm in F82H-std and about 4 nm in both F82H-2 and F82H-3. The number density of He bubbles was about two times higher than N_v. Swellings in F82H-std, F82H-2 and F82H-3 were 0.16, 0.33, and 0.38%, respectively.

In all alloys, voids arranged in lines were observed between dislocation lines. Voids were also observed on dislocation lines. Helium bubbles were formed preferentially on dislocation lines and also on dislocation loops and between dislocation lines. No voids were observed on lath boundaries. The number density of cavities in the region around the lath boundaries was lower than in the center region of lath cells. This cavity nucleation behavior was similar to that in F82H-std and F82H-2 irradiated to 7.4 dpa.

3.3. Microstructures of F82H-std irradiated to 51 dpa

Fig. 1(g) shows the cavities in F82H-std irradiated at 673 K to 51 dpa. On dislocation lines and between them, many faceted cavities and smaller cavities with diameters of 2–4 nm were observed. The size distribution of cavities had a peak at about 10-nm diameter, and the maximum diameter was 55 nm. The d^V_{RMC} and N_v were 22.0 nm and 5.0×10^{20} m^{-3}, respectively. Swelling was about 0.28%. The distribution of cavities was similar to that in the specimens irradiated to 7.4 and 26 dpa.

4. Discussion

4.1. Effect of He on number density of cavities

Cavity nucleation was assisted by He atoms, which was introduced by the transmutation reaction from $^{10}B(n,\alpha)^7Li$. The calculated He concentrations in F82H-std, F82H-2 and F82H-3 at 7.4 dpa were 6, 64, and 327 appm, respectively. The He atoms caused a large difference in cavity number density at 7.4 dpa. In F82H-3, which contained the highest concentration of He, the largest number density of cavities was observed. The size distribution of cavities in F82H-3 did not show a bimodal distribution, while those in F82H-std and F82H-2 showed a bimodal distribution. The number of He atoms in cavities was roughly estimated in all alloys with an assumption that He atoms were partitioned in observed defects such as He bubbles, voids, dislocations and lath boundaries according to their sink strengths [6]. The estimated number of He atoms in cavities in F82H-3 is much higher than that in He bubbles in F82H-std and F82H-2. It is believed that a bimodal size distribution was not observed in F82H-3 irradiated to 7.4 dpa because the number of He atoms in cavities was higher than the critical number [6].

After irradiation up to 26 dpa with a low He/dpa (0.32 appm He/dpa), the difference in the cavity number density among all alloys became small, but the F82H-3

had still the highest cavity number density. The size distribution of cavities in F82H-std and F82H-2 was still bimodal. The size distribution of cavities in F82H-3 changed from a mono-peak distribution at 7.4 dpa to a bimodal distribution at 26 dpa. Small cavities, 1.0–2.5 nm in diameter, were observed preferentially on dislocation lines in all alloys. These small cavities (He bubbles) seemed to nucleate after 7.4 dpa. It is believed that the cavity nucleation behavior was similar in all the alloys after 26 dpa, although the amount of ^{10}B was different in all alloys.

A few He bubbles were observed on lath boundaries in F82H-3 irradiated to 7.4 dpa. This specimen has a much higher He/dpa ratio (43 appm He/dpa) than other specimens. In other specimens, no cavities were observed on lath boundaries, even in F82H-3 irradiated to 26 dpa. The F82H-3 that has a high He/dpa ratio (12 appm He/dpa) at 26 dpa was severely damaged at a low He/dpa ratio after the burnout of ^{10}B (about 1 dpa). Farrell et al. [7] reported that He bubbles nucleated and grew on lath boundaries in Fe–9Cr–1Mo irradiated simultaneously with Ni, He and D ions at a constant rate of 10 appm He/dpa and 45 appm D/dpa. It is expected that under irradiation conditions of a high constant He/dpa ratio, He bubbles may nucleate on lath boundaries.

4.2. Effect of lath boundaries on cavity distribution

TEM observations revealed that no voids appeared on lath boundaries, and that the number density of cavities around lath boundaries was lower than in the center regions of lath cells. Swelling of F82H-std irradiated to ~51 dpa is plotted as a function of lath width in Fig. 2. The swelling was almost constant in lath cells with widths larger than 500 nm. As the width of the lath cells decreased to less than about 400 nm, swelling decreased rapidly. In the lath cells with widths smaller than about 200 nm, swelling was negligible. This was caused mainly by the reduction of N_v in smaller lath cells, although the d^V_{RMC} decreased slightly as the width of lath cells decreased. This was similar in all alloys in the dose range of this study. The average width of the lath cells in F82H was 300–400 nm. No large change in lath morphology in any specimen was observed after irradiation up to 51 dpa. Therefore, if all lath widths were smaller than about 200 nm, void swelling might be reduced to much lower levels. In alloys that contained the highest amount of ^{10}B, however, a relatively larger N_v was observed in small lath cells compared to alloys that contained the lowest amount of ^{10}B.

4.3. Dose dependence of swelling

As discussed above, swelling was affected by the width of lath cells. For the estimation of the dose dependence of swelling, lath cells with widths larger than 500 nm where swelling became constant were selected. Fig. 3 shows the dose dependence of swelling in F82H-std, F82H-2 and F82H-3 irradiated at 673 K up to 51 dpa with He concentrations between 6 and ~333 appm. For these conditions of displacement damage and He generation, swelling increased linearly with increasing displacement damage. In all alloys, the d^V_{RMC} decreased and N_v increased as a function of increasing displacement damage, respectively. Swelling of F82H-std is compared to the swelling of 7–10Cr ferrite/martensite steels irradiated at 663–703K [8–22] in Fig. 4. These swelling data were mainly obtained by fast reactor irradiation experiments. Swelling was measured by immersion density or TEM observations. The data obtained by TEM observations were measured in void-rich regions in the center of lath cells. The swelling in this study was in the same range as that from fast reactor irradiation experiments, although the swelling data from the fast reactor experiment show a considerable scatter. This similarity may occur because the He/dpa ratio in

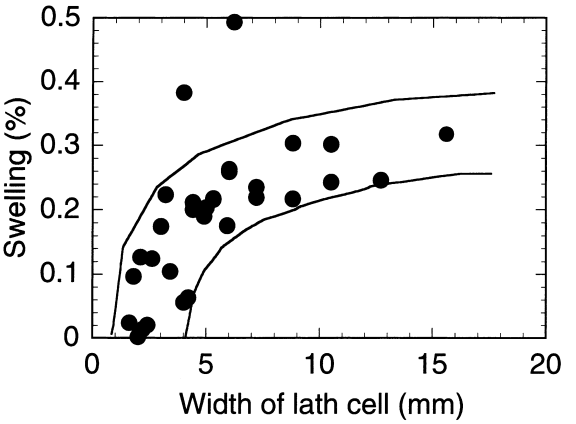

Fig. 2. Dependence of swelling on lath width in F82H-std irradiated at 673 K to 51 dpa.

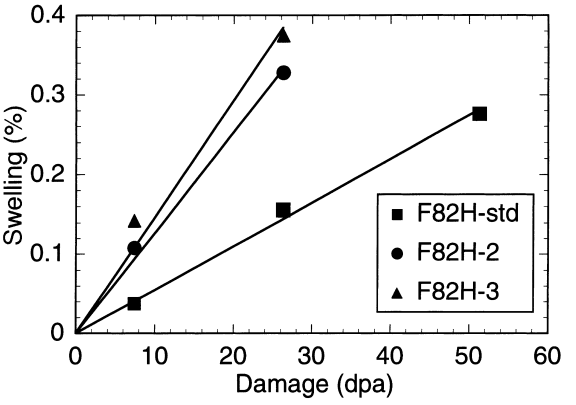

Fig. 3. Dose dependence of swelling in F82H-std, F82H-2 and F82H-3 irradiated at 673 K up to 51 dpa.

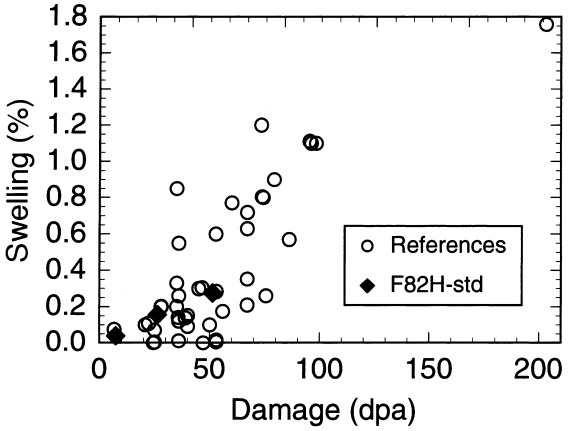

Fig. 4. Swelling of F82H-std (◆) and 7–10Cr ferritic/martensitic steels (○) irradiated at 663–703 K.

this experiment (~0.32 appm He/dpa) is not too different from that of the fast reactor experiments (~0.08 appm He/dpa in FFTF).

5. Conclusions

F82H-std and variants of this alloy doped with isotopically tailored boron were irradiated at about 673 K up to about 51 dpa in HFIR. The concentration of ^{10}B in these alloys was 4, 62, and 325 appm. After irradiation, TEM observation was performed and the following conclusions were made:

1. Swelling of F82H-std and the two alloys doped with ^{10}B increased linearly with increasing displacement damage. The average diameter of voids increased and the number density of voids decreased with increasing displacement damage.
2. With the addition of ^{10}B, the number density of cavities increased. Larger swelling was observed in alloys containing higher concentrations of ^{10}B.
3. Voids were observed on dislocation lines and between dislocation lines, but not on the lath boundaries.

Acknowledgements

The authors would like to thank Dr R.L. Klueh for helpful discussions, Mr L.T. Gibson for preparation of radioactive specimens and members of the Bldg. 3025E Hot Cell Facility for their support. This research was supported in part by an appointment (NH) to the Oak Ridge National Laboratory Postdoctoral Associates Program administered jointly by the Oak Ridge National Laboratory and the Oak Ridge Institute for Science and Education. The research is also sponsored by the Office of Fusion Energy Science, US Department of Energy, under contract DE-AC05-96OR22464 with the Lockheed Martin Energy Research Corporation.

References

[1] A. Hishinuma, A. Kohyama, R.L. Klueh, D.S. Gelles, W. Dietz, K. Ehrlich, J. Nucl. Mater. 258–263 (1998) 193.
[2] P.J. Maziasz, R.L. Klueh, J.M. Vitek, J. Nucl. Mater. 141–143 (1986) 929.
[3] K. Shiba, M. Suzuki, A. Hishinuma, J.E. Pawel, ASTM-STP 1270 (1996) 753.
[4] L.R. Greenwood, Fusion Reactor Materials Semiannual Progress Report, DOE/ER-313/23, 1997, p. 301.
[5] L.R. Greenwood, Fusion Reactor Materials Semiannual Progress Report, DOE/ER-313/23, 1997, p. 305.
[6] L.L. Horton, L.K. Mansur, ASTP-STP 870 (1985) 344.
[7] K. Farrell, E.H. Lee, ASTM-STP 870 (1985) 383.
[8] A. Kimura, M. Narui, H. Kayano, J. Nucl. Mater. 191–194 (1992) 879.
[9] A. Kimura, H. Matsui, J. Nucl. Mater. 212–215 (1994) 701.
[10] A. Kimura, T. Moriyama, M. Narui, H. Matsui, J. Nucl. Mater. 233–237 (1996) 319.
[11] T. Moriyama, A. Kimura, H. Matsui, J. Nucl. Mater. 239 (1996) 118.
[12] P.J. Maziasz, R.L. Klueh, J.M. Vitek, J. Nucl. Mater. 141–143 (1986) 929.
[13] D.S. Gelles, J. Nucl. Mater. 233–237 (1996) 293.
[14] D.S. Gelles, J. Nucl. Mater. 103&104 (1981) 975.
[15] R.W. Powell, D.T. Peterson, M.K. Zimmerschied, J.F. Bates, J. Nucl. Mater. 103&104 (1981) 969.
[16] J.J. Kai, R.L. Klueh, J. Nucl. Mater. 230 (1996) 116.
[17] E.A. Little, J. Nucl. Mater. 206 (1993) 324.
[18] Y. Kohno, A. Kohyama, M. Yoshino, K. Asakura, J. Nucl. Mater. 212–215 (1994) 707.
[19] T. Shibayama, A. Kimura, H. Kayano, J. Nucl. Mater. 233–237 (1996) 270.
[20] P.J. Maziasz, R.L. Klueh, ASTM-STP 1046 (1989) 35.
[21] Y. Kohno, D.S. Gelles, A. Kohyama, M. Tamura, A. Hishinuma, J. Nucl. Mater. 191–194 (1992) 863.
[22] D. Gilbon, J.L. Séran, R. Cauvin, A. Fissolo, A. Alamo, F. Le Naour, V. Lévy, ASTM-STP 1046 (1989) 5.